Types of Fulde-Ferrell-Larkin-Ovchinnikov states induced by anisotropy effects

Dmitry Denisov and Alexander Buzdin*
Condensed Matter Theory Group, CPMOH, University of Bordeaux, 351 Cours de la Liberation, F-33405 Talence, France

Hiroshi Shimahara
Department of Quantum Matter Science, ADSM, Hiroshima University, Higashi-Hiroshima 739-8530, Japan
(Received 17 November 2008; published 4 February 2009)

The crystal structure determines both the Fermi surface and pairing symmetry of the superconducting metals. It is demonstrated in the framework of the general phenomenological approach that this is of primary importance for the determination of the structure of the Fulde-Ferrell-Larkin-Ovchinnikov (FFLO) phase in the magnetic field. The FFLO modulation of the superconducting order parameter may be revealed in the form of the higher Landau-level states or/and modulation along the magnetic field. The transition between different FFLO states could occur with the temperature variation or with the magnetic field rotation.

DOI: 10.1103/PhysRevB.79.064506 PACS number(s): 74.81.−g, 74.25.Dw

I. INTRODUCTION

It is well known that in type II superconductors the Abrikosov vortex state can be formed under a magnetic field. In most cases the destruction of superconductivity happens due to the orbital effect. However there can be a situation when paramagnetic effect plays an important role in destruction of superconductivity (magnetic field acting only on electron spins). In this case the nonuniform Fulde-Ferrell-Larkin-Ovchinnikov (FFLO) state[1,2] appears in superconductors, which is characterized by the modulation of the order parameter. The structure of the FFLO phase in real compounds may be very rich.[3–12] Interplay of orbital and paramagnetic effects has been described in the isotropic model by Gruenberg and Gunther in Ref. 3, where they calculated critical field and structure of the order parameter. It was found in Ref. 3 that the orbital effect is detrimental to the FFLO state, but still such state can exist if the ratio of pure orbital effect $H_{c2}^{\mathrm{orb}}(0)$ and pure paramagnetic limit $H_p(0)$ is larger than 1.28, i.e., the Maki parameter $\alpha_M=\sqrt{2}H_{c2}^{\mathrm{orb}}(0)/H_p(0)$ must be larger than 1.8. Pure paramagnetic limit at $T=0$ can be estimated as $H_p(0)=\Delta_0/\sqrt{2}\mu_B$, where Δ_0 is the BCS gap at $T=0$ and μ_B is the Bohr magneton. In Ref. 3 the modulation was studied using a zero Landau-level function, which holds true only for moderate Maki parameter $\alpha_M<9$. It was found in Ref. 4 that for large values of Maki parameter $\alpha_M>9$ the higher Landau-level solutions become relevant. In this case the critical field $H_{c2}(T)$ consists of several curves each corresponding to a different Landau-level solution. The analyses of the orbital effect in the FFLO state[3,4] were performed for the isotropic metals with *s*-wave type of pairing. However in Ref. 13 it was demonstrated that it is readily generalized for the case of the metals with elliptic Fermi surface.

In such a case the Maki parameter becomes angular dependent. For example, for the case of the quasi-two-dimensional (2D) or anisotropic three-dimensional (3D) superconductors, α_M increases dramatically for the in-plane field orientation. Therefore we may expect transitions between the usual FFLO state with zero Landau levels[3] and the state with higher Landau levels[4–7] when the magnetic field is tilted from the perpendicular orientation to the parallel one. Also crossover from the pure FFLO state to the vortex states with higher Landau-level indexes in the model of quasi-2D system has been predicted in Ref. 14. In real compounds the deviation of the Fermi surface from the elliptic form is crucial for the adequate description of the FFLO state as well as the type of the superconductivity pairing (e.g., *s* or *d* wave).[15–17] This circumstance is related with the fact that the description of the FFLO state in the framework of Ginzburg-Landau approach needs the consideration of the higher-order derivatives of the order parameter in addition to the usual gradient terms. For example, in the case of pure paramagnetic effect the critical field and modulation vector q strongly depend on anisotropy or nesting properties of the Fermi surface.[18–21] In this paper we consider a realistic case with a nonelliptic Fermi surface, and for definiteness we restrict ourselves to the tetragonal symmetry. For example, quasi-two-dimensional superconductor $CeCoIn_5$ (Ref. 9) provides favorable conditions for the formation of the FFLO state and it has a tetragonal symmetry.

A characteristic feature of the FFLO state is the existence of a tricritical point (TCP) in the field-temperature phase diagram.[22] TCP is the meeting point of three transition lines separating the normal metal, the uniform superconductivity, and the FFLO state. Formation of the FFLO state near the TCP may be described by modified Ginzburg-Landau (MGL) functional.[23] Appearance of the nonuniform state is related with a change in the sign of the coefficient g at the gradient term $g|\Pi_i\Psi|^2$ in the free-energy density. In the standard Ginzburg-Landau theory the coefficient g is positive. Here it vanishes at the TCP $[T^*,H_{c2}(T^*)]$ and then becomes negative for $T<T^*$. The absolute value of g grows as we move further from the TCP, for example, with increasing of the magnetic field or lowering temperature. A negative g means that the modulated state has a lower free energy than the uniform one. In order to obtain the modulation vector one needs to include the term with higher-order derivatives in the MGL functional.[23]

In this paper we study the effects of crystal (or pairing) anisotropy on the FFLO phase. Using MGL approach we introduce free-energy density $\mathcal{F}$ describing the tetragonal system. We examine the case of the Fermi surface close to the elliptic one. Therefore $\mathcal{F}$ can be divided into isotropic

and perturbative parts. We demonstrate that the higher Landau-level solutions may be realized for arbitrary values of Maki parameter in contrast to isotropic model. This is a special mechanism of the higher Landau-level phase formation in 3D system. Moreover depending on various types of deviation of the Fermi surface from isotropic form, three possible solutions for the FFLO state can be realized: (a) maximum modulation occurs along the magnetic field with zero Landau-level state, (b) both modulation and higher Landau-level state, and (c) highest possible Landau level and no modulation along the field (or modulation with very small wave vector). Moreover due to the specific form of the Fermi surface the variation in magnetic field orientation may provoke transitions between the states with different Landau levels.

The main goal of the present paper is to demonstrate that in the presence of the orbital effect and for the realistic Fermi surface, the very different types of the FFLO state could be realized. In particular, if the preferred modulation direction is perpendicular to the magnetic field, this can result in the formation of the higher Landau-level mixed state with no modulation along the field at all. Our approach is fully justified near the TCP and for superconductors with large Maki parameters. However, qualitatively, it provides the understanding of the FFLO state at all temperatures and for arbitrary strength of the orbital effect. Here we calculate the line of the second-order transition from the normal to the superconducting state. For this purpose we use the quadratic over the superconducting order-parameter MGL functional. To describe the properties of the FFLO state it is needed to retain the higher-order terms over the superconducting order parameter. The situation is completely analogous with that of the Abrikosov vortex lattice. From the symmetry reasons it is clear that the transitions between the mixed states describing the different Landau levels will be the first-order transitions. However the appearance of the modulation along the magnetic field may occur through a continuous transition. All these interesting questions deserve further studies but they are well beyond the scope of the present paper.

II. FFLO STATE IN ANISOTROPIC GINZBURG-LANDAU MODEL

The most general form of the MGL functional quadratic over Ψ is

$$\mathcal{F}=\alpha|\Psi|^2-\sum_{i=1}^{3} g_i|\Pi_i\Psi|^2+\sum_{i=1}^{3}\gamma_i|\Pi_i^2\Psi|^2+\sum_{i\neq j}\varepsilon_{ij}|\Pi_i\Pi_j\Psi|^2, \tag{1}$$

where $\alpha(H,T)=\alpha_0[T-T_{cu}(H)]$, $T_{cu}(H)$ is the transition temperature into the uniform superconducting state, $\Pi_i=-i\hbar\frac{\partial}{\partial x_i}-\frac{2e}{c}A_i$ are momentum operators, and A_i are the components of the vector potential; further we set $\hbar=1$. Assuming the tetragonal symmetry in the case of the pure elliptic Fermi surface, we have the following relation for the effective mass $m_z\neq m_x=m_y=m$. The elliptical Fermi surface could be transformed into the isotropic one by the following scaling transformation $z'=\sqrt{m_z/m}z$.[13] Components of the magnetic field also transform as $H\rightarrow H'=(\sqrt{\frac{m}{m_z}}H_x,\sqrt{\frac{m}{m_z}}H_y,H_z)$. Further we suppose that actual Fermi-surface deviation from the elliptical form is small, and after the corresponding scaling transformation functional (1) for the tetragonal symmetry is written as

$$\mathcal{F}=\alpha|\Psi|^2-g\sum_{i=1}^{3}|\Pi_i\Psi|^2+\gamma\left|\sum_{i=1}^{3}\Pi_i^2\Psi\right|^2+\varepsilon_z|\Pi_z^2\Psi|^2+\frac{\varepsilon_x}{2}(|\Pi_x\Pi_y\Psi|^2+|\Pi_y\Pi_x\Psi|^2)+\frac{\tilde{\varepsilon}}{2}(|\Pi_z\Pi_x\Psi|^2+|\Pi_x\Pi_z\Psi|^2+|\Pi_z\Pi_y\Psi|^2+|\Pi_y\Pi_z\Psi|^2). \tag{2}$$

Coefficients $g,\gamma,\varepsilon_z,\varepsilon_x,\tilde{\varepsilon}$ depend on structure of the Fermi surface, but for the FFLO appearance g must be positive. The terms $-g\Sigma_{i=1}^{3}|\Pi_i\Psi|^2+\gamma|\Sigma_{i=1}^{3}\Pi_i^2\Psi|^2$ describe the elliptic form of the Fermi surface (for s-wave superconductivity), and terms with coefficients ε_z, ε_x, and $\tilde{\varepsilon}$ are considered as perturbation.

Without orbital effect the momentum operators are simplified to $\Pi_i=-i\frac{\partial}{\partial x_i}$ and the solution for the order parameter could be presented as $\Psi=\Psi_q\exp(i\vec{q}\cdot\vec{r})$. In the case of elliptic Fermi surface we have a degeneracy over direction of the FFLO modulation q. The crystal structure effects are expressed via the terms with ε_z, ε_x, and $\tilde{\varepsilon}$, and they lift this degeneracy and determine the direction of the FFLO modulation. The free-energy density is written as

$$\mathcal{F}=\sum_q\{\alpha-gq^2+\gamma q^4+\varepsilon_z q^4\cos^4\theta+\varepsilon_x q^4\sin^4\theta\cos^2\varphi\sin^2\varphi+\tilde{\varepsilon}q^4\sin^2\theta\cos^2\theta\}|\Psi_q|^2, \tag{3}$$

where we have used the spherical system for $\vec{q}$: $q_x=q\cos\varphi\sin\theta$, $q_y=q\sin\varphi\sin\theta$, and $q_z=q\cos\theta$. Due to the tetragonal symmetry the modulation in xy plane is either parallel to the x or y axis ($\varepsilon_x>0$) or along the bisector ($\varepsilon_x<0$). For definiteness we may suppose that $\varepsilon_x>0$. Note that in the case $\varepsilon_x<0$ the rotation of the xy axis by $\pi/4$ provides us the same functional (3) with renormalized coefficients ε_z' and $\tilde{\varepsilon}'$ but with $\varepsilon_x>0$. The wave vector of modulation q will be in the xy plane if $\tilde{\varepsilon}>2\varepsilon_z$, $\varepsilon_z<0$; it is parallel to the z axis if $\tilde{\varepsilon}>0$, $\varepsilon_z>0$ (see Fig. 1). For the region $\tilde{\varepsilon}<0$, $\tilde{\varepsilon}<2\varepsilon_z$, the direction of modulation is at angle $\theta=\frac{1}{2}\arccos\frac{\varepsilon_z}{(\tilde{\varepsilon}-\varepsilon_z)}$ to the z axis. Therefore the crystal anisotropy (or/and pairing anisotropy) lifts the degeneracy over the direction of the FFLO modulation and the whole diagram in the $(\varepsilon_z,\tilde{\varepsilon})$ plane is presented in Fig. 1.

III. ORBITAL EFFECT FOR THE MAGNETIC FIELD APPLIED ALONG THE z AXIS

The exact solution of the linearized equation for $\Psi(\vec{r})$ is unavailable in the general case if the orbital effect is taken into account. The Landau-level solution with additional

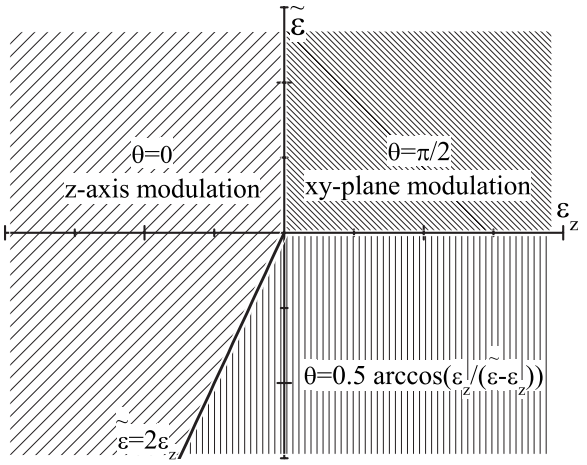

FIG. 1. Modulation $(\tilde{\varepsilon},\varepsilon_z)$ diagram in the case of the absence of the orbital effect (pure paramagnetic limit). Areas with different patterns correspond to different orientations of the wave-vector modulation. The phase diagram does not depend on the ε_x value.

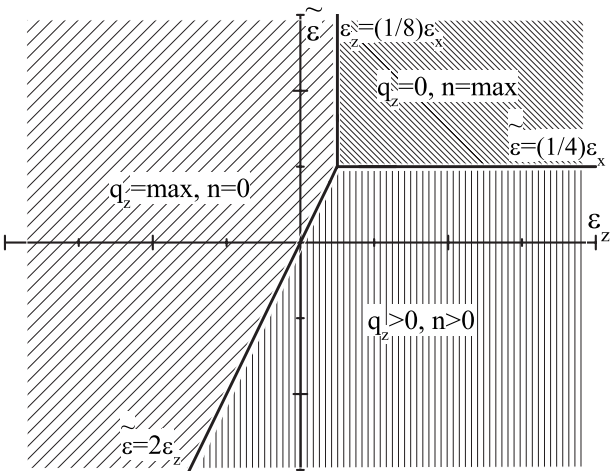

FIG. 2. Modulation diagram in the case when the magnetic field is applied along the z axis. There are three areas on the diagram corresponding to three types of solution for modulation vector q_z and Landau level n. Modulation direction is always parallel to the applied field, and ε_x here is chosen equal to γ.

modulation along the field works only for the case of elliptical Fermi surface. In this case we obtain the degeneracy over modulation q and Landau level n when we move from the TCP. However if the anisotropy effects are taken into account they lift this degeneracy. We demonstrate that depending on the parameters of the system very different types of the FFLO state could be realized.

We begin with the case where magnetic field H is applied along the tetragonal z axis and the gauge is chosen as $A=(yH,0,0)$. Following, for example, Ref. 7 we can express our operators Π_i using boson operators of creation η and annihilation η^+ as $\Pi_x=i\frac{1}{\sqrt{2}\xi_H}(\eta-\eta^+)$ and $\Pi_y=\frac{1}{\sqrt{2}\xi_H}(\eta+\eta^+)$, where $\xi_H=\sqrt{\frac{c}{2eH}}$. Our goal is to find $T_c(H)$, which is the transition temperature into the FFLO state, i.e., we need to find the solution which gives the maximum of $\alpha(H,T)=\alpha_0[T_c-T_{\mathrm{cu}}(H)]$. To do this we use the variation method[24] and look for a maximum of α written as

$$\alpha(H,T)=\max\left\{\frac{\int[\alpha|\Psi|^2-\mathcal{F}]d^3r}{\int|\Psi|^2d^3r}\right\}. \tag{4}$$

In the general case $\Psi(x,y,z)=\Sigma C_n\varphi_n(x,y)e^{iq_zz}$, but since the anisotropy effects are small we can approximate our solution only with a single Landau-level function φ_N,[25] which is a well-known solution for the system with isotropic form of the Fermi surface. In our calculations we use the following properties of Landau functions: $\int\varphi_n\varphi_m d^3r=\delta_{nm}$, $\eta\varphi_n=\sqrt{n}\varphi_{n-1}$, and $\eta^+\varphi_n=\sqrt{n+1}\varphi_{n+1}$; we also normalize C_n so that $\int|\Psi|^2d^3r=1$. To neglect the other Landau-level functions $(n\neq N)$ in our Ψ representation, their corresponding coefficients should be small compared to the coefficient C_N. This leads to the following condition for the applicability of the single-level approximation $\xi_H^{-2}\gg\frac{g}{\gamma}\sqrt{\frac{\varepsilon}{\gamma}}$ which is determined by the Fermi-surface deviation ε from the elliptic form (ε is of the order of average among $\tilde{\varepsilon}$, ε_z, and ε_x and its exact value depends on magnetic field orientation). Calculating $\alpha(H,T)$ using the operators η and η^+ we can express it in terms of q_z and $\xi_n^{-2}=\xi_H^{-2}(2n+1)$ as

$$\alpha(H,T)=\max\left\{g[q_z^2+\xi_n^{-2}]-\gamma[q_z^2+\xi_n^{-2}]^2-\varepsilon_zq_z^4-\varepsilon_x\frac{1}{8}\xi_n^{-4}-\tilde{\varepsilon}q_z^2\xi_n^{-2}-\varepsilon_x\frac{5}{8}\xi_H^{-4}\right\}. \tag{5}$$

If we consider only the unperturbed part $g[q_z^2+\xi_n^{-2}]-\gamma[q_z^2+\xi_n^{-2}]^2$, set $u=q_z^2+\xi_n^{-2}$, and take the derivative with respect to u, we obtain the maximum point at $u_0=g/2\gamma$. When the system is close to the TCP, g is small so that $g/2\gamma<\xi_H^{-2}$. In this case we obtain the lowest Landau level $n=0$ and no modulation along z $(q_z=0)$. If we move further from the TCP and g grows $(\xi_H^{-2}<g/2\gamma<3\xi_H^{-2})$ then n remains equal to 0 but q_z does not. If Maki parameter is large then our approach will still be valid even far away from the TCP. In this case $g/2\gamma\geq3\xi_H^{-2}$ and n can be larger than 0. Hence, we have degeneracy over choosing of Landau level n and q_z. But as was written earlier taking into account small perturbative terms with $\varepsilon_z,\varepsilon_x,\tilde{\varepsilon}$ we remove this degeneracy and find the maximum $\alpha(H,T)$ with a respect to $q_z=\sqrt{u_0-\xi_n^{-2}}$. There are three possible types of solutions (combinations of n and q_z) depending on $\varepsilon_z,\varepsilon_x,\tilde{\varepsilon}$: (a) maximum modulation $q_z=\sqrt{g/2\gamma-\xi_H^{-2}}$ and zero Landau level n; (b) nonzero modulation $q_z=\sqrt{\frac{g}{2\gamma}(\varepsilon_x-4\tilde{\varepsilon})/(8\varepsilon_z+\varepsilon_x-8\tilde{\varepsilon})}$ with $n=\mathrm{int}\{\frac{1}{2}[\xi_H^2(u_0-q_z^2)-1]\}$, where int means that only the integer part is taken; and (c) highest possible Landau level $n=\mathrm{int}[\frac{g}{4\gamma}\xi_H^2-\frac{1}{2}]$ and near-zero modulation. All these cases are shown in Fig. 2. However due to integer nature of n the modulation q_z has a very special behavior in cases (b) and (c); it changes abruptly everytime our solution jumps from one to another Landau level. It should be noted that in case (c) the wave vector of modulation q_z instead of being zero oscillates with H (or with g when we move further form the

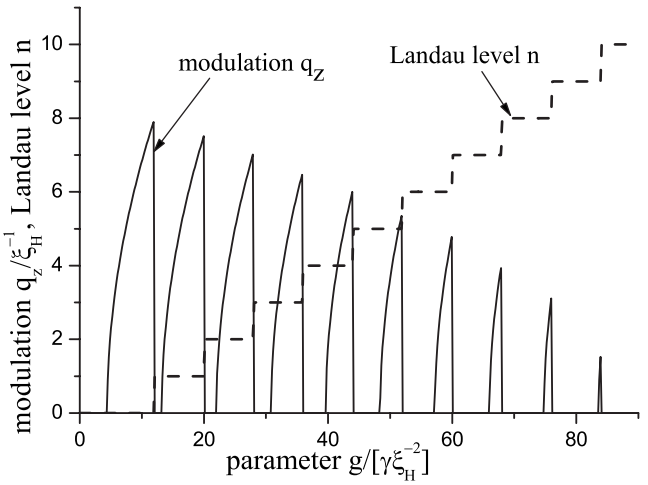

FIG. 3. Dependence of residual modulation on the parameter g (normalized to $\gamma\xi_H^{-2}$). The wave vector of modulation q is shown here by the solid line and measured in units of ξ_H^{-1}. The values of Landau level n is shown by the dashed line. The parameter $\tilde{\varepsilon}$ is chosen here as 0.2γ.

TCP) due to the mismatch of $u_0=g/2\gamma$ and $\xi_n^{-2}=\xi_H^{-2}(2n+1)$. The diagram shown in Fig. 2 looks similar to that in Fig. 1 with the exception of the shift along both axes due to the presence of the ε_x coefficient. When we get zero wave vector of modulation in Fig. 2 the same area in Fig. 1 corresponds to modulation in the xy plane. If the modulation vector q along the applied magnetic field is zero then modulation could arise in the direction perpendicular to the field. When n and q_z are intermediate (not maximum and not zero; lower-right part of the diagrams), FFLO modulation could be formed in both perpendicular and parallel directions to the field $(q_\parallel^2+q_\perp^2=g/2\gamma-\xi_H^{-2})$. It should be noted that we cannot achieve a smooth transition from one diagram to another by decreasing H to 0 due to the condition of single Landau-level approximation $\xi_H^{-2}\gg\frac{g}{\gamma}\sqrt{\frac{\varepsilon}{\gamma}}$, despite the fact that the only difference between the diagrams in Figs. 1 and 2 is the shift of the intersection point due to the presence of the ε_x coefficient. The same is true for the case $H\|x$ where difference will be more significant.

Maximum Landau level and residual modulation. Due to the fact that n is an integer the wave vector of modulation q_z may not be exactly equal to zero but to some value less than $\sqrt{u_0-\xi_n^{-2}}$ when n is maximum. To calculate this value we maximize $\alpha(H,T)$ from Eq. (5) again but this time $\xi_n^{-2}=\xi_H^{-2}(2n+1)$ will be treated as a constant. We obtain $q_z^2=\max(0,\frac{u_0-\xi_n^{-2}-(\tilde{\varepsilon}/2\gamma)\xi_n^{-2}}{1+(\varepsilon_z/\gamma)})$ and the general solution for residual modulation q_z will oscillate with H or with g (absolute value of g is increasing when we are moving away from the TCP). Wave vector of modulation is zero when ξ_n^{-2} is close to $u_0=g/2\gamma$, then it starts to increase linearly with g until it drops to zero again when the solution "jumps" to another Landau level (Fig. 3). With the increasing effect of anisotropy, the area of zero wave-vector modulation widens, and in the limiting case it will cover all parameter ranges. Similar results were obtained for the isotropic case at $\alpha_M>9$ at low temperature.[4]

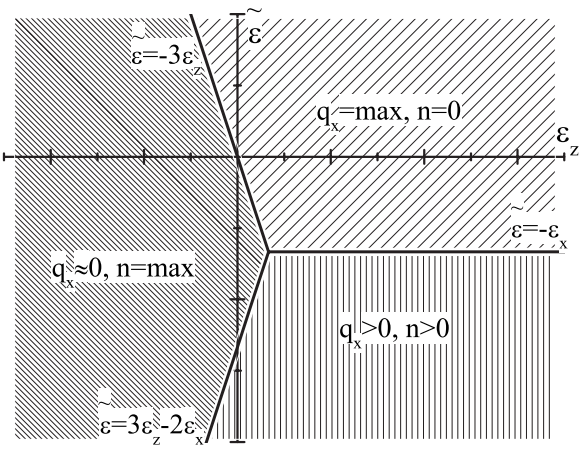

FIG. 4. Modulation diagram $(\tilde{\varepsilon},\varepsilon_z)$ in the case when the magnetic field is applied along the x axis. There are three areas on the diagram corresponding to different types of solution for modulation vector q_x and Landau level n. Modulation direction is always parallel to the applied field. The position of the intersection point is determined by the coefficient ε_x.

IV. CASE OF THE MAGNETIC FIELD APPLIED ALONG THE x AXIS

For magnetic field applied along the x axis we choose $\vec{A}$ as $(0,0,yH)$, the order parameter $\Psi(x,y,z)=\varphi_N(y)e^{iq_x x}$, where q_x is modulation along the x axis, and reintroduce creation and annihilation operators as $\eta=\frac{\xi_H}{\sqrt{2}}(\Pi_y-i\Pi_z)$ and $\eta^+=\frac{\xi_H}{\sqrt{2}}(\Pi_y+i\Pi_z)$. Repeating the same calculations as for the $H\|z$ case we have

$$\alpha(H,T)=\max\left\{g[q_x^2+\xi_n^{-2}]-\gamma[q_x^2+\xi_n^{-2}]^2-\varepsilon_z\frac{3}{8}\xi_n^{-4}-\frac{1}{2}\varepsilon_x q_x^2\xi_n^{-2}-\frac{1}{2}\tilde{\varepsilon}q_x^2\xi_n^{-2}-\tilde{\varepsilon}\frac{1}{8}\xi_n^{-4}-\varepsilon_z\frac{3}{8}\xi_H^{-4}-\tilde{\varepsilon}\frac{5}{8}\xi_H^{-4}\right\}. \quad (6)$$

Again we set $u=q_x^2+\xi_n^{-2}$ and find that the maximum point $u_0=g/2\gamma$ is the same for unperturbed part. The degeneracies over q_x and n are removed in a similar way by taking into account the perturbative terms $\varepsilon_z,\varepsilon_x,\tilde{\varepsilon}$. Diagram for maxima of $\alpha(H,T)$ in the case with magnetic field applied along the x axis is shown in Fig. 4. Three main areas of the diagrams are similar to the ones shown in Fig. 2: (a) maximum modulation $q_x=\sqrt{g/2\gamma-\xi_H^{-2}}$ and zero Landau level n; (b) nonzero modulation $q_x=\sqrt{\frac{g}{2\gamma}(3\varepsilon_z-\tilde{\varepsilon}-2\varepsilon_x)/(3\varepsilon_z-3\tilde{\varepsilon}-4\varepsilon_x)}$ with $n=\mathrm{int}\{\frac{1}{2}[\xi_H^2(u_0-q_x^2)-1]\}$; and (c) highest possible Landau level $n=\mathrm{int}[\frac{g}{4\gamma}\xi_H^2-\frac{1}{2}]$ and residual modulation described earlier. Diagrams shown in Figs. 1 and 4 have some similarities with a respect to the conditions for the different types of solutions. On both diagrams the FFLO modulation along the x (or y) axis corresponds to the upper-right quarter and there is no modulation in the xy plane in the left quarters of the diagrams.

V. MAGNETIC FIELD APPLIED IN THE *xy* PLANE

If a magnetic field H is applied in the xy plane (β is the angle between $\vec{H}$ and x axis), then it is convenient to rotate the x and y axes around z by angle β to reduce the problem to the case $H\|x$. Under this rotation the terms with coefficients g, γ, and ε_z remain unchanged and the rest parts are transformed according to rules $x'=x\cos\beta+y\sin\beta$, $y'=y\cos\beta-x\sin\beta$,

$$\Pi_x = \Pi_x'\cos\beta - \Pi_y'\sin\beta, \tag{7}$$

$$\Pi_y = \Pi_x'\sin\beta + \Pi_y'\cos\beta, \tag{8}$$

$$\Pi_z = \Pi_z' = -i\frac{\partial}{\partial z} - \frac{2e}{c}y'H. \tag{9}$$

The operators η and η^+ are expressed using the new Π_x', Π_y', and Π_z' as before in the case $H\|x$. Due to the symmetry of the problem only the ε_x term in Eq. (2) acquires the dependence on β in the final expression for $\alpha(H,T)$,

$$\alpha(H,T) = \max\Bigg\{ g[q_x'^2+\xi_n^{-2}] - \gamma[q_x'^2+\xi_n^{-2}]^2 - \varepsilon_z\frac{3}{8}\xi_n^{-4} - \frac{1}{2}\varepsilon_x q_x'^2\xi_n^{-2} - \varepsilon_x\frac{\sin^2 2\beta}{4}\Bigg(q_x'^4 - 3q_x'^2\xi_n^{-2} + \frac{3}{8}\xi_n^{-4} + \frac{3}{8}\xi_H^{-4}\Bigg) - \frac{1}{2}\tilde{\varepsilon}q_x'^2\xi_n^{-2} - \tilde{\varepsilon}\frac{1}{8}\xi_n^{-4} - \varepsilon_z\frac{3}{8}\xi_H^{-4} - \tilde{\varepsilon}\frac{5}{8}\xi_H^{-4}\Bigg\}, \tag{10}$$

where q_x' is the modulation along the new x' axis parallel to the magnetic field H. Directly from the ε_x term it can be concluded that the angles $\beta=0,\pm\frac{\pi}{2},\pi$ will lead to the old results when magnetic field is applied along the x or y axis. The main results for the maximum of $\alpha(H,T)$ will be similar to the case $H\|x$, with the only exception that separation lines on phase diagram are changed to three lines: $\tilde{\varepsilon}=-3\varepsilon_z+\frac{5}{4}\sin^2 2\beta\varepsilon_x$, $\tilde{\varepsilon}=3\varepsilon_z+(\frac{15}{4}\sin^2 2\beta-2)\varepsilon_x$, and $\tilde{\varepsilon}=(\frac{5}{2}\sin^2 2\beta-1)\varepsilon_x$. However this change only affects the initial shift of the diagram from the center. For example in Fig. 5 the case $\beta=\frac{\pi}{2}(n+\frac{1}{2})$ is shown and the intersection point has shifted to the opposite quarter of the graph. For general values of β, the intersection point is situated at $(\varepsilon_z,\tilde{\varepsilon})=[(-\frac{5}{12}\sin^2 2\beta+\frac{1}{3})\varepsilon_x,(\frac{5}{2}\sin^2 2\beta-1)\varepsilon_x]$ on a line segment connecting the two intersection points for $\beta=\frac{\pi}{2}n$ and $\beta=\frac{\pi}{2}(n+\frac{1}{2})$. On the phase diagram like in previous cases we have three possible solutions. (1) $q_x'^2=u_0(3\varepsilon_z-\tilde{\varepsilon}-2\varepsilon_x+\frac{15}{4}\sin^2 2\beta\varepsilon_x)/(3\varepsilon_z-3\tilde{\varepsilon}-4\varepsilon_x+\frac{35}{4}\sin^2 2\beta\varepsilon_x)$ and $n=\mathrm{int}\{\frac{1}{2}[\xi_H^2(u_0-q_x'^2)-1]\}$ when $\tilde{\varepsilon}<\min[3\varepsilon_z-2\varepsilon_x+\frac{15}{4}\sin^2 2\beta\varepsilon_x,\ \varepsilon_x(\frac{5}{2}\sin^2 2\beta\varepsilon_x-1)]$. (2) $q_x'\approx 0$ (near-zero residual modulation) and the maximum n in this case will be equal to $\mathrm{int}[\frac{g}{4\gamma}\xi_H^2-\frac{1}{2}]$. This corresponds to $-3\varepsilon_z+\frac{5}{4}\sin^2 2\beta\varepsilon_x>\tilde{\varepsilon}>3\varepsilon_z-2\varepsilon_x+\frac{15}{4}\sin^2 2\beta\varepsilon_x$. (3) $q_x'=\sqrt{g/2\gamma-\xi_H^{-2}}$—maximum modulation along the magnetic field with $n=0$. This corresponds to $\tilde{\varepsilon}>\max[\varepsilon_x(\frac{5}{2}\sin^2 2\beta\varepsilon_x-1),-3\varepsilon_z+\frac{5}{4}\sin^2 2\beta\varepsilon_x]$.

Using q_x' corresponding to the maximum of $\alpha(H,T)$ we find $T_c(H)$. When the parameters of our system (the actual values of $\tilde{\varepsilon},\varepsilon_z,\varepsilon_x$ coefficients) correspond to the point in the $(\tilde{\varepsilon},\varepsilon_z)$ plane situated near one of the separation lines in Fig. 4 or Fig. 5 then the magnetic field rotation can lead to transition between the corresponding two phases. The simplest case with $\tilde{\varepsilon}=0$, $\varepsilon_z=0$, is shown in Figs. 6 and 7. For positive ε_x the transition is between states $(q=0,\ n=\max)$ and $(q>0,\ n>0)$; for negative ε_x the two states are $(q=\max,\ n=0)$ and $(q>0,\ n>0)$. The integer nature of Landau level n manifests itself in the state $(q>0,\ n>0)$ when the FFLO modulation could change several Landau levels while magnetic field rotates in a given region. In this case T_c line consists of several curves each corresponding to a different Landau-level solution. If switching between the different solutions does not occur then the general T_c dependence will be reduced to the simple sinusoidal form with period $\pi/2$.

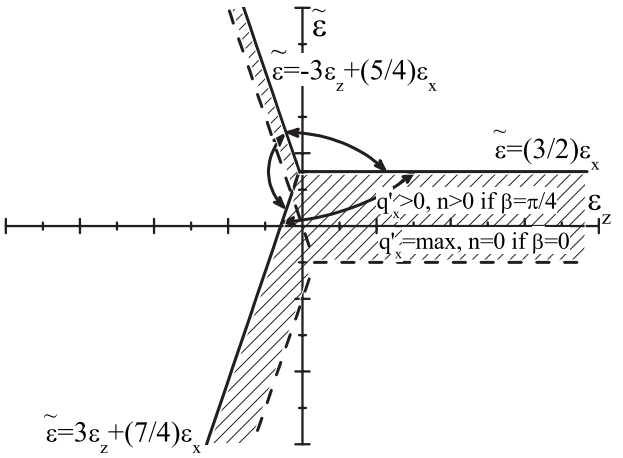

FIG. 5. Modulation diagram in the case when the magnetic field is applied in the xy plane. Solid separation lines correspond to the case of $\beta=\pi/4$ and dashed lines to the case of $\beta=0$. Patterned area corresponds to the region where the type of the solution for q and n could be changed during rotation along the z axis.

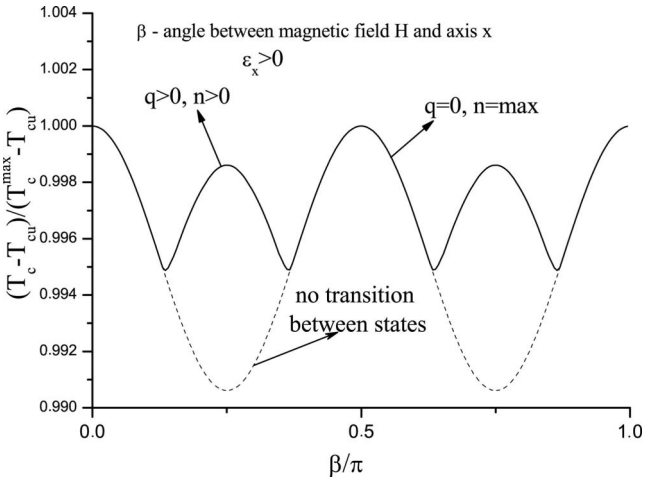

FIG. 6. Transition temperature dependence on the angle β of the magnetic field in the xy plane. For illustration we have chosen $\varepsilon_z=\tilde{\varepsilon}=0$, $\varepsilon_x=0.1\gamma$, and g (normalized to $\gamma\xi_H^{-2}$) equal to 100. There are switchings between two types of the solution: $(q>0,\ n>0)$ and $(q=0,\ n=\max)$.

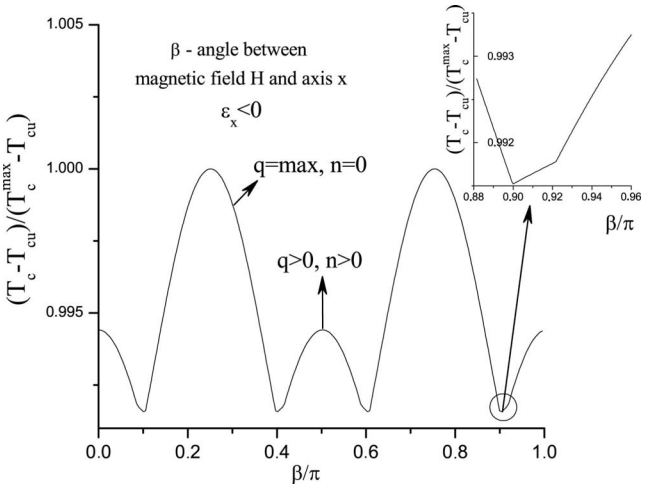

FIG. 7. Transition temperature dependence on the angle β of the magnetic field in the xy plane. For illustration we have chosen $\varepsilon_z = \tilde{\varepsilon} = 0$, $\varepsilon_x = -0.1\gamma$, and g (normalized to $\gamma\xi_H^{-2}$) equal to 40. There are switchings between two types of the solution: $(q>0,\ n>0)$ and $(q=\max,\ n=0)$. The inset shows magnification of the region near switching point. T_c line consists of several curves each corresponding to a different Landau level n ($n=0$, 1, and 2 in this case).

VI. CUBIC SYMMETRY

In the case of cubic symmetry ε_z is equal to 0 and $\tilde{\varepsilon} = \varepsilon_x = \varepsilon$. In the absence of the orbital effect the direction of modulation will be along one of the axes if $\varepsilon > 0$ and along one of the main diagonals if $\varepsilon < 0$. In the presence of orbital effect when magnetic field is applied along one of the cubic axes, the type of solution for maximum $\alpha(H,T)$ depends only on the sign of ε. If $\varepsilon < 0$ then q is equal to $\sqrt{\frac{3}{7}}u_0$ and $n = \mathrm{int}[\frac{2}{7}\xi_H^2 u_0 - \frac{1}{2}]$. For $\varepsilon > 0$ there will be the choice between highest and zero modulations. If $u_0 > 7\xi_H^{-2}$ then we obtain the maximum modulation along the field $q = \sqrt{u_0 - \xi_H^{-2}}$ and Landau level n will be zero. But when $u_0 < 7\xi_H^{-2}$ it is more favorable to have zero (or some residual due to the mismatch) modulation q and highest Landau level $n = \mathrm{int}[\frac{1}{2}\xi_H^2 u_0 - \frac{1}{2}]$. In the latter case when the modulation along the field is absent $(q \approx 0)$ it turns out that the maximum Landau level cannot be higher than 3. In the case with the magnetic field applied along one of the diagonals we have the same situation but with the opposite sign of ε. Note that in all these cases the momentum and Landau level do not depend on ε at the first approximation.

VII. DISCUSSION

We investigated the influence of the crystal structure effects on the FFLO state based on the modified Ginzburg-Landau approach. We analyzed the possible solutions for the FFLO modulation vector and relevant Landau-level functions. We have used the single-level approximation, but we believe that qualitatively our results would remain valid even if we take into account the general multilevel representation of the order parameter. For illustration we have restricted ourselves to the tetragonal symmetry because the most promising material for FFLO realization $CeCoIn_5$ has, namely, this type of symmetry. Our results can be easily generalized to any symmetry as long as deviation of the Fermi surface from the elliptic form can be treated as a perturbation. In the opposite case the single-level Landau function solution will be transformed into a series of higher-level functions. Also this will lead to the broadening of the $q=0$ region shown in Fig. 3, which means that for a wide range of parameters in such a case there will be no more modulation along the field. The form of the Fermi surface determines the direction of the FFLO modulation in the pure paramagnetic limit. We see that in the presence of the orbital effect the system tries in some way to reproduce these optimal directions of the FFLO modulation by varying the Landau-level index n and wave vector of the modulation along the field.

The higher Landau-level solutions has been predicted for the FFLO phase in 2D superconductors in tilted magnetic field,[5–7] in 3D d-wave and quasi-2D s- and d-wave superconductors,[11,27] and in 3D isotropic superconductors at low temperature provided that the Maki parameter is large.[4] Here we have demonstrated that for certain field orientations such states naturally appear in real 3D compounds in a whole region of the FFLO phase existence (without any restriction to the value of Maki parameter). This behavior is related with crystal structure and/or pairing symmetry effects. The isotropic models used so far to describe FFLO state fail to predict these different types of scenarios of the FFLO transitions. Indeed following the isotropic (or quasi-isotropic) model the transition to the FFLO state with the increase in the magnetic field always occurs via the modulation appearance along the field direction. On the contrary in the present paper we predict the FFLO transition as a formation of the higher Landau-level states. The vortex state that corresponds to these higher Landau-level solutions have a rather complicated structure due to the competition between two length scales—the average distance between vortices and the FFLO period.[12,26,28] Recently in Ref. 29 the very special vortex phases with spatial line nodes forming a variety of 3D spatial configurations have been predicted. Therefore we may expect that the mixed state in the FFLO superconductor may be very different from the usual Abrikosov lattice, provided that the higher Landau-level solutions are realized. The experimentally verified consequences of these scenario of the FFLO transition are the first-order transitions between the states with different Landau-level solutions (namely, between $n=0$ and $n=1$), accompanied by the strong change in the vortex lattice structure. The standard experimental techniques of the vortex lattice observation (including the neutron scattering) could be used to detect these transformations.

It is commonly believed that the FFLO state in $CeCoIn_5$ corresponds to the state with the modulation along the magnetic field for both field orientations: along the tetragonal axis and in the basal plane. However, comparing the $(\tilde{\varepsilon}, \varepsilon_z)$ diagrams (Figs. 2 and 4) we see that the situation when we have a zero Landau-level solution for this two field orientations is improbable. In $CeCoIn_5$ the crystal structure effects are rather important—for example in Ref. 30 the vortex lattice reorientation transition has been reported as well as in-plane anisotropy of the upper critical field.[31] In such a case we can expect that for one of these field orientations the Landau-level solution with $n \geq 1$ may be realized. Note that

such a possibility in connection with the FFLO state in $CeCoIn_5$ has been discussed in Ref. 32. If the crystal structure effects are large enough for the Landau-level solutions with $n \geq 1$, the modulation along the field may be absent. Very recently[33] the modulated antiferromagnetic ordering has been reported in the low-temperature superconducting phase of $CeCoIn_5$ at the magnetic field in the basal plane. The antiferromagnetic ordering plays for the FFLO state the role of the crystal structure effect favoring the orientation of the FFLO modulation wave vector along the antiferromagnetic one.[13] The texture in the superconducting order parameter revealed by NMR experiments looks different for different field orientations[9] as well as the anomaly in the local magnetic inductor measurements.[34] This may indicate the different types of the FFLO state for different field orientations. Presumably for the field orientation in the basal plane there are no FFLO modulations along the field.

ACKNOWLEDGMENTS

The authors are grateful to Y. Matsuda, T. Shibauchi, J. P. Brison, J. Flouquet, J. Cayssol, and F. Konschelle for useful discussions and comments. This work was supported by ANR Extreme Conditions Correlated Electrons under Grant No. ANR-06-BLAN-0220 (for D.D. and A.B.) and by University Bordeaux 1 (for H.S.).

*Also at Institut Universitaire de France, Paris, France.
[1] P. Fulde and R. A. Ferrell, Phys. Rev. **135**, A550 (1964).
[2] A. I. Larkin and Yu. N. Ovchinnikov, Zh. Eksp. Teor. Fiz. **47**, 1136 (1964) [Sov. Phys. JETP **20**, 762 (1965)].
[3] L. W. Gruenberg and L. Gunther, Phys. Rev. Lett. **16**, 996 (1966).
[4] A. I. Buzdin and J. P. Brison, Phys. Lett. A **218**, 359 (1996).
[5] A. I. Buzdin and J. P. Brison, Europhys. Lett. **35**, 707 (1996).
[6] L. N. Bulaevskii, Zh. Eksp. Teor. Fiz. **65**, 1278 (1973) [Sov. Phys. JETP **38**, 634 (1974)].
[7] H. Shimahara and D. J. Rainer, J. Phys. Soc. Jpn. **66**, 3591 (1997).
[8] M. Ichioka, H. Adachi, T. Mizushima, and K. Machida, Phys. Rev. B **76**, 014503 (2007).
[9] Y. Matsuda and H. Shimahara, J. Phys. Soc. Jpn. **76**, 051005 (2007).
[10] H. Shimahara, J. Phys. Soc. Jpn. **67**, 736 (1998).
[11] H. Shimahara, S. Matsuo, and K. Nagai, Phys. Rev. B **53**, 12284 (1996).
[12] U. Klein, D. Rainer, and H. Shimahara, J. Low Temp. Phys. **118**, 91 (2000); U. Klein, Phys. Rev. B **69**, 134518 (2004).
[13] J. P. Brison, N. Keller, A. Vernière, P. Lejay, L. Schmidt, A. Buzdin, J. Flouquet, S. R. Julian, and G. G. Lonzarich, Physica C **250**, 128 (1995).
[14] H. Shimahara, in *The Physics of Organic Superconductors and Conductors*, edited by A. G. Lebed (Springer, New York, 2008).
[15] M. Houzet and V. P. Mineev, Phys. Rev. B **74**, 144522 (2006).
[16] A. Buzdin, Y. Matsuda, and T. Shibauchi, Europhys. Lett. **80**, 67004 (2007).
[17] F. Konschelle, J. Cayssol, and A. I. Buzdin, Europhys. Lett. **79**, 67001 (2007).
[18] H. Shimahara, J. Phys. Soc. Jpn. **66**, 541 (1997).
[19] H. Shimahara, J. Phys. Soc. Jpn. **68**, 3069 (1999).
[20] H. Shimahara and S. Hata, Phys. Rev. B **62**, 14541 (2000).
[21] H. Shimahara and K. Moriwake, J. Phys. Soc. Jpn. **71**, 1234 (2002).
[22] D. Saint-James, G. Sarma, and E. J. Thomas, *Type II Superconductivity* (Pergamon, New York, 1969).
[23] A. I. Buzdin and H. Kachkachi, Phys. Lett. A **225**, 341 (1997).
[24] A. A. Abrikosov, *Fundamentals of the Theory of Metals* (Elsevier, Netherlands, 1988).
[25] L. D. Landau and E. M. Lifshitz, *Quantum Mechanics: Nonrelativistic Theory* (Pergamon, Oxford, 1977).
[26] Y. Suginishi and H. Shimahara, Phys. Rev. B **74**, 024518 (2006).
[27] M. Houzet and A. Buzdin, Europhys. Lett. **50**, 375 (2000).
[28] K. Yang and A. H. MacDonald, Phys. Rev. B **70**, 094512 (2004).
[29] D. F. Agterberg, Z. Zheng, and S. Mukherjee, Phys. Rev. Lett. **100**, 017001 (2008).
[30] L. DeBeer-Schmitt, C. D. Dewhurst, B. W. Hoogenboom, C. Petrovic, and M. R. Eskildsen, Phys. Rev. Lett. **97**, 127001 (2006).
[31] F. Weickert, P. Gegenwart, H. Won, D. Parker, and K. Maki, Phys. Rev. B **74**, 134511 (2006).
[32] H. A. Radovan, N. A. Fortune, T. P. Murphy, S. T. Hannahs, E. C. Palm, S. W. Tozer, and D. Hall, Nature (London) **425**, 51 (2003).
[33] M. Kenzelmann, Th. Strässle, C. Niedermayer, M. Sigrist, B. Padmanabhan, M. Zolliker, A. D. Bianchi, R. Movshovich, E. D. Bauer, J. L. Sarrao, and J. D. Thompson, Science **321**, 1652 (2008).
[34] R. Okazaki, H. Shishido, T. Shibauchi, M. Konczykowski, A. Buzdin, and Y. Matsuda, Phys. Rev. B **76**, 224529 (2007).